Blends of a PPO–PS Alloy with a Liquid Crystalline Polymer

R. VISWANATHAN and A. I. ISAYEV*

Department of Polymer Engineering, The University of Akron, Akron, Ohio 44325-0301

SYNOPSIS

Blends of a PPO–PS alloy with a liquid crystalline polymer have been studied for their dynamic properties, rheology, mechanical properties, and morphology. This work is an extension of our previous work on PPO/LCP blends. The addition of the LCP to the PPO–PS alloy resulted in a marked reduction in the viscosity of the blends and increased processibility. The dynamic studies showed that the alloy is immiscible and incompatible with the LCP at all concentrations. The tensile properties of the blends showed a drastic increase with the increase in LCP concentration, thus indicating that the LCP acted as a reinforcing agent. The tensile strength, secant modulus, and impact strength of the PPO–PS/LCP blends were significantly higher than that of PPO/LCP blends. Morphology of the injection molded samples of the PPO–PS/LCP blends showed that the *in situ* formed fibrous LCP phase was preserved in the solidified form. A distinct skin–core morphology was also seen for the blends, particularly with low LCP concentrations. The improvement of the mechanical properties of the blends is attributed to these *in situ* fibers of LCP embedded in the PPO–PS matrix. The improvement in the properties of PPO–PS/LCP over PPO/LCP is also attributed to the addition of the PS which consolidates the matrix. © 1995 John Wiley & Sons, Inc.

INTRODUCTION

A number of studies have been performed in recent years in the blending of thermoplastics with a liquid crystalline polymer.[1–13] Liquid crystalline polymer (LCP) is a unique material for blending with other thermoplastics because of its outstanding mechanical properties and relative chemical inertness. The high strength of the LCP results from the molecular orientation in the nematic phase during processing. This leads to the formation of rigid, rod-like structures extended in the machine direction. Thus when the LCP is blended with a thermoplastic in an elongational and shear field, highly fibrillar structures of LCP domains in the thermoplastic matrix are obtained. This leads to *in situ* reinforcement of the thermoplastic. The *in situ* reinforcement helps circumvent processing problems that are encountered in the case of conventional reinforcing materials such as glass, carbon fibers, etc. However, molded products made from thermoplastic/LCP blends, as well as pure LCP, are deficient in one respect: their properties are highly anisotropic. The strength and modulus are significantly higher in the machine direction than the transverse direction, owing to fiber formation in the machine direction.

Poly(phenylene oxide)–polystyrene (PPO–PS) alloys are some of the most widely used engineering thermoplastics. PS is completely miscible with PPO in all proportions.[14] PPO itself has a glass transition temperature of around 210°C. Addition of PS reduces the glass transition temperature of PPO. A wide range of different types of PPO–PS alloys are available, depending upon the amount of PS in the system. Thus, selectivity is one of the advantages of using PPO–PS alloys for a variety of applications. High strength at elevated temperatures and low density make the alloys ideal for applications where strength-to-weight ratio is important. PPO–PS alloys exhibit excellent dimensional stability and chemical resistance, and thus are possibly good choices for blending with LCP.

Blends of polycarbonate and LCPs based on hydroxy benzoic acid (HBA)/hydroxy napthoic acid (HNA) have been studied by Isayev and Modic.[12] The studies have shown that the LCP acts as an

* To whom correspondence should be addressed.

Journal of Applied Polymer Science, Vol. 55, 1117–1129 (1995)
 CCC 0021-8995/95/071117-13

effective processing aid for polycarbonate. ICI patent[13] states that a small amount of LCP reduces the viscosity of the flexible polymer. Thus the LCP acts not only as an *in situ* reinforcing agent but also as a processing aid when blended with thermoplastics. Recently, several papers related to the blends of PPO/LCP were published where the effect of self-reinforcement was achieved.[11,16]

This paper is an extension of our previous work on PPO/LCP blends.[2] The results from the studies on the miscibility, rheology, mechanical properties, and morphology of a blend of an LCP with a PPO–PS alloy has been presented. The purpose of the present study is to determine the similarities and differences in properties between the PPO/LCP and PPO–PS/LCP blends.

MATERIALS AND METHOD OF INVESTIGATION

The materials used in the study were an alloy of PPO and PS (Noryl 731, General Electric) and a thermotropic LCP based on HBA/HNA (Vectra A950, Hoechst Celanese). Blends of Noryl and LCP of various concentrations were prepared by extrusion, using a twin-screw extruder (ZSK-30, Werner and Pfleiderer), and subsequently pelletized. The blends contained 10%, 25%, 40%, 50%, 60%, 75%, and 90% LCP in the system. The temperature of all zones of the extruder were maintained at 275°C and the speed was set at 140 rpm.

End-gated, dumbbell-shaped bars of two sizes, *viz.* 0.155 × 0.0125 × 0.0033 m (standard tensile bars, or STBs) and 0.063 × 0.0031 × 0.0015 m (mini tensile bars, or MTBs) were injection-molded using a Boy 15S Screw Injection Molding Machine. The injection molding conditions are provided in Table I. The MTBs were used for mechanical testing and DMTA measurements.

Table I Injection Molding Conditions for PPO–PS/LCP Blends

Barrel Temperature (all Zones)	: 275°C
Nozzle Temperature	: 100%
Mold Temperature	: 120°C
Clamping Force	: 24 tons
Injection Pressure	: 13.79 MPa (2000 psi)
Back Pressure	: 0.48 MPa (70 psi)
Injection Speed	: 4.6×10^{-5} m^3/s
Holding Time	: 15–20 sec
Screw Speed	: 250–260 RPM

The dynamic mechanical properties were measured using a Dynamic Mechanical Thermal Analyzer (Polymer Laboratories). The temperature sweep employed was 30°C to 250°C and the heating rate was 4°C/min. The tests were performed in a single cantilever bending mode using the MTBs. The tests were carried out at a frequency of 1 Hz and a peak-to-peak displacement of 6.4×10^{-5} m, using a medium size clamp B. Readings of storage and loss modulus along with tan δ values were recorded. The transition temperatures for the PPO–PS/LCP blends, taken from pellets, were obtained using a Differential Scanning Calorimeter (DuPont, model 9900) in a nitrogen atmosphere. A heating rate of 20°C/min. was employed and a 10 mg sample of Indium was used for calibration.

Viscosity measurements were made using an Instron Capillary Rheometer (Instron, model 3211) with a long capillary die of 0.00127 m diameter and a L/D ratio of 28.7 at 275°C. The flow curves were obtained without the entrance pressure corrections.

The mechanical properties of the blends were obtained using an MTS mechanical tester capable of a cyclic operation (Model 305.03, serial number 62). Hydraulic clamps of the MTS tester allowed firmer hold on the samples under a pressure of 2–3 MPa. A triangular mode of operation with a very slow head movement (0.01–0.11 Hz frequency) converted the fatigue tester into a stress-strain tester, since the MTBs tended to break during the extension period of the cycle. Moreover, the compression period of the cycle placed the head in the exact same starting position, thus contributing to the consistency of the tests. The results were obtained through a microprocessor (MTS microconsole 458.20) and the peak tensile strength could be read directly from the microprocessor. A chart recorder was used to record the movement of the head and the readings obtained were used to calculate the secant modulus and elongation to break (secant modulus is defined as the modulus of the sample at 1% elongation). The crosshead speed was set at 5 mm/min. and the chart speed was set at 20 cm/min. The impact strength of the samples was obtained by using an Izod Impact Tester (Testing Machines, Inc.) with a 5 lb hammer. The STBs were cut to 0.0635 m length and notched according to ASTM D235C standards.

The morphologies of the blends were studied using a scanning electron microscope (SEM ISI SX-40). The MTBs of the various blends were immersed in liquid nitrogen and flexed to fracture. The samples were mounted on sample-holders with a quick-drying cyanoacrylate and then coated with a gold-palladium alloy using a Polaron SEM coating machine. The coating time was fixed at 60 seconds.

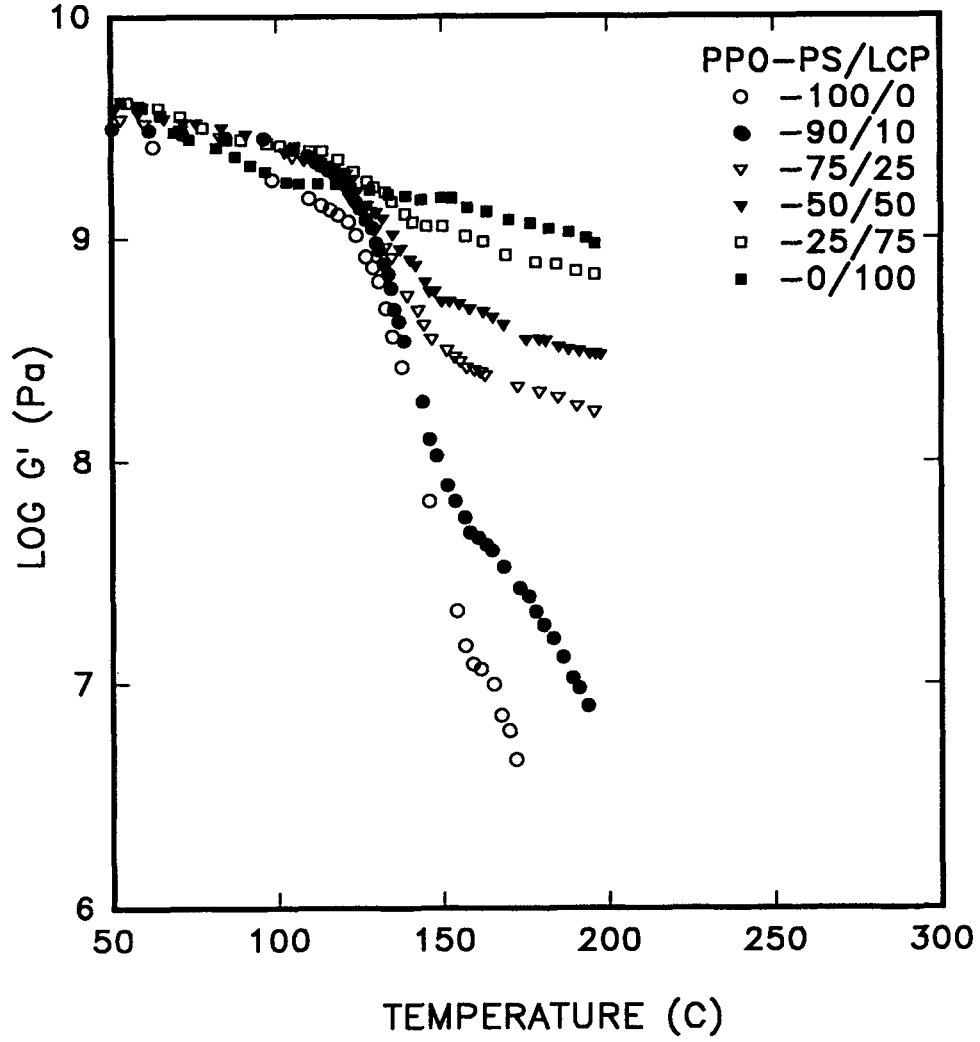

Figure 1 Storage modulus (G') as a function of temperature for PPO–PS/LCP blends.

RESULTS AND DISCUSSION

Miscibility Studies

DMTA and DSC studies were performed to understand the miscibility of the blends of PPO–PS with the LCP. The DMTA is a versatile tool to study the crystallinity, miscibility, and phase separation in the case of blends, particularly at elevated temperatures.[15] Figures 1, 2, and 3 give the storage modulus, the loss modulus, and the tan δ values against temperature, respectively. The plots indicate that there is a transition from a glassy state to a rubbery state with the progressive heating of the sample. The transition occurs around 150°C for the PPO–PS/LCP blends. The significant features from the figures are the increase in the storage modulus and a decrease in the tan δ values with the increase in the LCP content in the blends. The peak of tan δ for pure PPO–PS occurs around 150°C, and slightly drops with the addition of LCP, indicating the T_g of the blends. The peak of tan δ decreases significantly with the increase in the LCP content; this has been observed earlier for other thermoplastic/LCP blends.[6,12,16] The loss modulus also passes through a maxima at a temperature below the T_g, as seen in Figure 2. For majority of the blends, the T_g of the LCP cannot be seen from these curves. However, for high LCP concentrations and pure LCP, T_g is around 100°C. Earlier studies[7,12] have shown that there exists a second transition zone at high temperature corresponding to the melting of the LCP. The present study, however, focuses more on the glass transitions of the matrix polymer (PPO–PS) as affected by blending with the LCP.

The substantial decrease in the peak value of

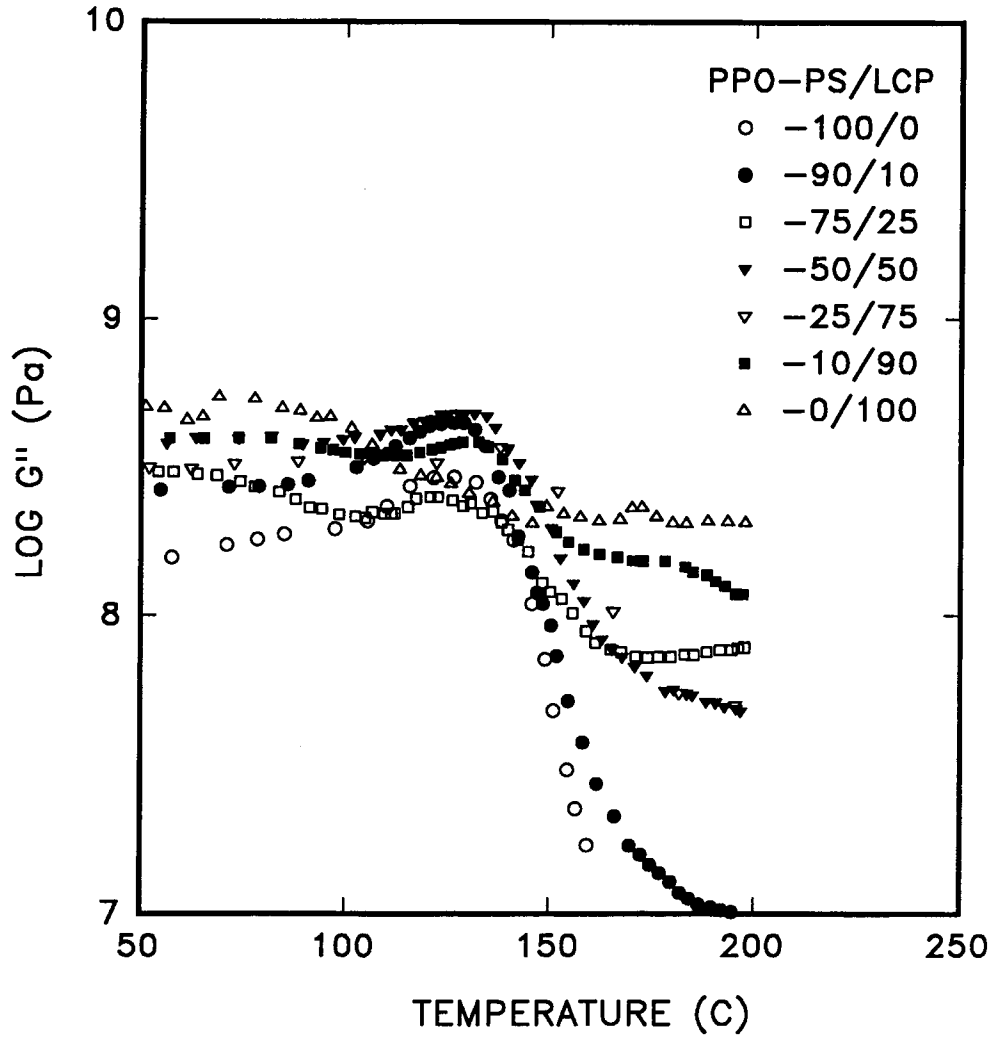

Figure 2 Loss modulus (G'') as a function of temperature for PPO–PS/LCP blends.

tan δ with the increase in the LCP concentration can be attributed to the incorporation of crystalline LCP domains in an otherwise amorphous PPO–PS domain, leading to decrease in the mobility of the chains in the amorphous regions. In the case of PPO/LCP blends,[16] the storage modulus, loss modulus, and tan δ values follow a trend similar to that in this study, although the peaks are around 200°C. Miscible blends show T_gs that are in between those of pure components. There are no distinct peaks for PPO and PS in the case of PPO–PS/LCP blends. This is because the PS is completely miscible with PPO at all concentrations and does not phase separate in the presence of the LCP. A distinct peak of tan δ for the LCP seen at 100°C weakens with the decrease in the LCP concentration in the blend. There is distinct tan δ peaks for PPO–PS in the blend, regardless of the LCP concentration in the blend. This shows that the PPO–PS and LCP are immiscible at all concentrations of LCP in the blends. There is a slight downward shift of the tan δ peaks in the temperature scale with the change in concentration of LCP in the blends in both PPO/LCP studied by Limtasiri and Isayev[16] and PPO–PS/LCP blends of the present study. This conclusion is further supported by the morphological studies described below.

The observations made using the DMTA analysis are further augmented by the differential scanning calorimetry. Figure 4 gives the heat flow as a function of time. It can be seen from the figure that there are two distinct transitions corresponding to the T_g of the two components. It can be seen that the increase in the concentration of PPO–PS leads to a very slight shift of T_g. This shows that the two components are, in general, immiscible and incompati-

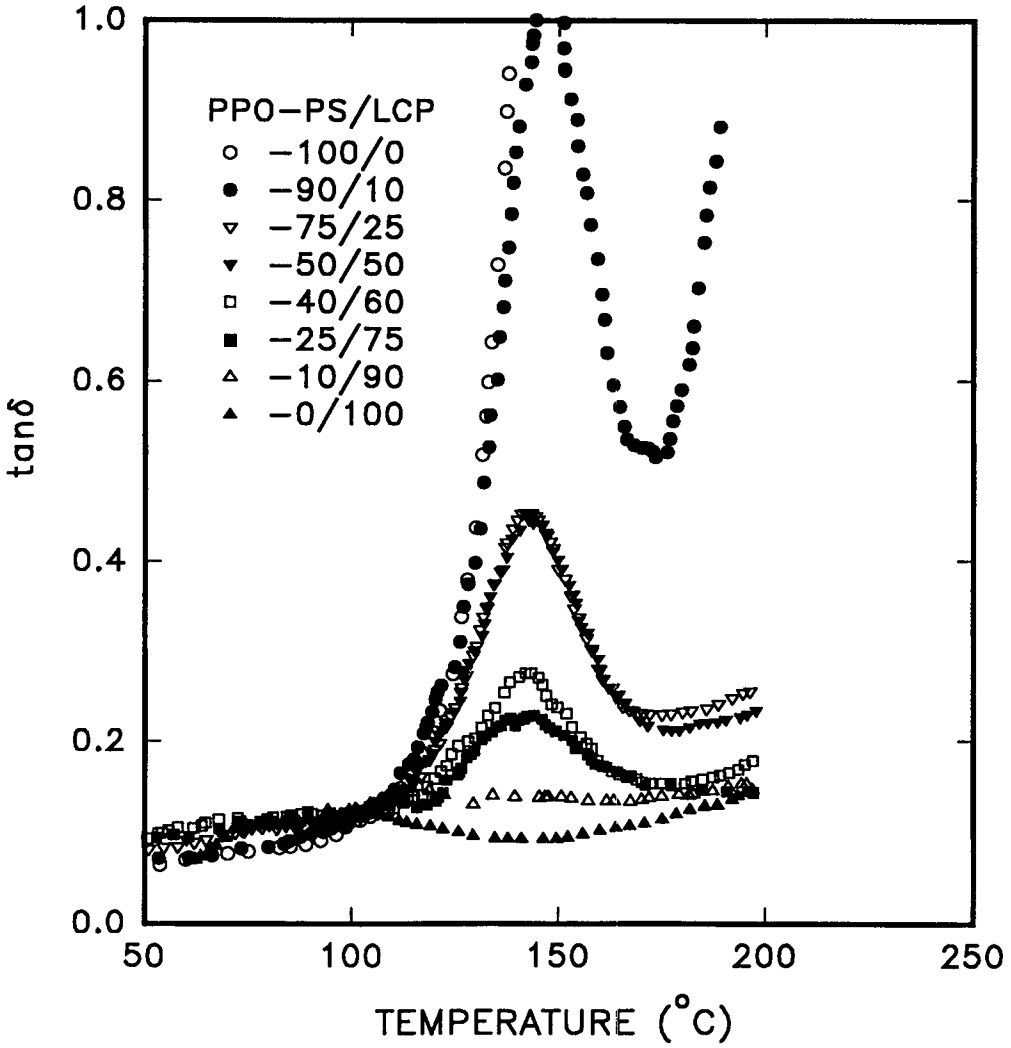

Figure 3 Tan δ as a function of temperature for PPO–PS/LCP blends.

ble. Similar results have been seen in the case of PC/LCP,[12] PEI/LCP,[7] PEEK/LCP,[17] and PPO/LCP[16] blends.

Rheological Properties

Figure 5 gives the viscosity vs. shear rate for various concentrations of PPO–PS/LCP blends at 275°C. Studies have indicated that the addition of LCP to a thermoplastic results in the reduction in the viscosity of the blend.[12,13] From Figure 5, it can be seen that the viscosity of PPO–PS/LCP blends also decreases with an increase in LCP content. It can be seen from Figure 6 that for blends with an LCP concentration greater than 50%, the blend viscosity is less than that of either of the components. A similar trend has been observed in the case of PPO/LCP blends[16] and PEEK/LCP blends.[6] The decrease in viscosity is highly conspicuous at higher shear rates where the non-newtonian behavior is predominant. The reduction in viscosity can be attributed to the orientation of LCP and inherent stiffening of the fibers in the flow direction. The oriented fibers are presumed to slide past one another, leading to lubrication of the melt and thus a reduction in melt viscosity.[8] Again the interfacial slippage between the two polymers may also be a reason for the reduction in the viscosity.[18] Migration of the LCP to the wall of the capillary could also cause the reduction in viscosity. This is not a major factor, however, since at high LCP concentrations, the viscosity of the blends is lower than that of pure LCP.

Studies on blends of two thermoplastics have shown that the fibrillation is maximum when the viscosity ratio of the dispersed polymer and the matrix polymer approaches unity.[19] This occurs at the crossover point between the flow curves of the two components of the blend. In the case of PPO–PS/

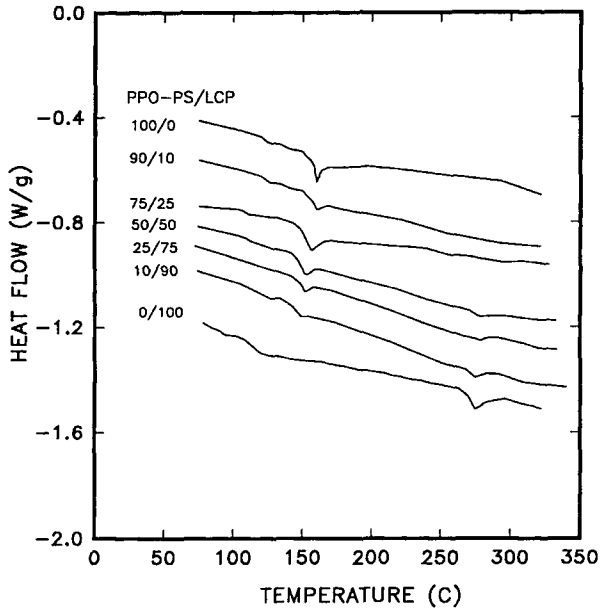

Figure 4 DSC thermograms for PPO–PS/LCP blends at a heating rate of 20°C/min.

LCP blends, the crossover point occurs at very low shear rates, as seen in Figure 5. But in the case of blends involving LCPs, the maximum fibrillation occurs at much higher shear rates where the viscosity ratio of the matrix to fiber phase is greater than unity. This has been seen for PC/LCP[12] and PEI/LCP[7] systems.

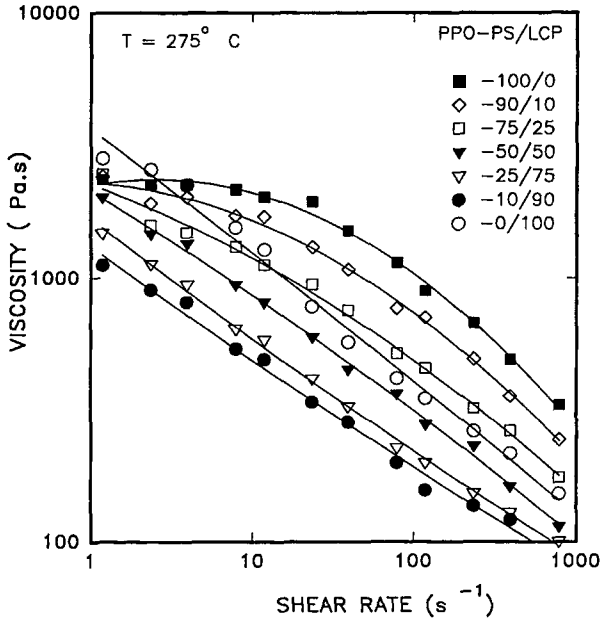

Figure 5 Viscosity vs. shear rate for PPO–PS/LCP blends at a temperature of 275°C.

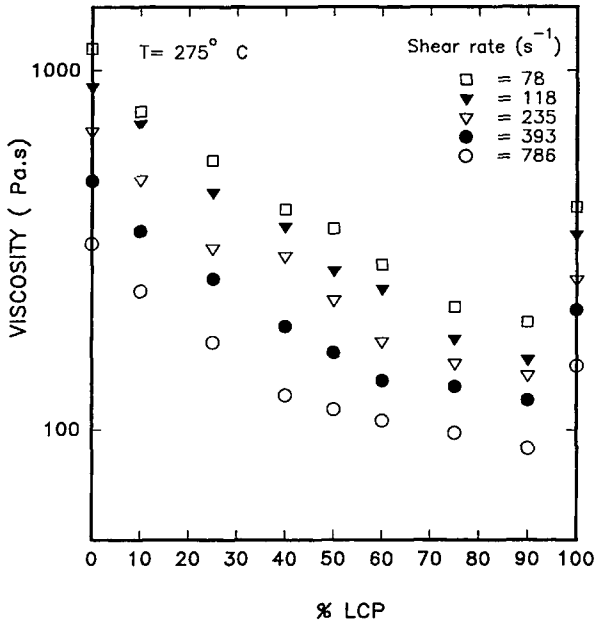

Figure 6 Viscosity vs. LCP concentration for PPO–PS/LCP blends at various shear rates at a temperature of 275°C.

Figure 7 uses the Heitmiller equation[20] to compare the viscosity of the blend as a function of LCP concentration with the theoretically predicted values. The Heitmiller equation can be given as follows:

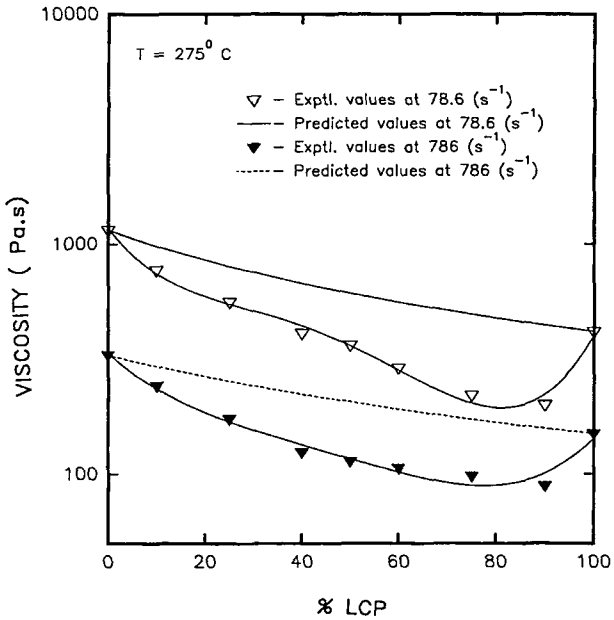

Figure 7 Experimental and predicted viscosity vs. LCP concentration for PPO–PS/LCP blends at shear rates of 78.6 s^{-1} and 786 s^{-1}. The predicted values were obtained by using Heitmiller's equation.

$$\frac{1}{\eta_b} = \frac{\phi_1}{\eta_1} + \frac{\phi_2}{\eta_2} \quad (1)$$

where η_b is the viscosity of the blend, η_1 and η_2 are the viscosities of the individual components, and ϕ_1 and ϕ_2 are the volume fractions of the individual components. It can be seen that the theoretically predicted values for the PPO–PS/LCP blends have a positive deviation from the experimental curve. This shows that the viscosity reduction in the case of PPO–PS/LCP blends is synergistic and the decrease is greater for higher amounts of LCP in the blend. This decrease in viscosity is important, particularly for thermoplastics that have processing problems due to high viscosity. The addition of LCP, even in small quantities, could significantly reduce the viscosity of the blend and aid in processing.

The difference between the experimental and calculated viscosities, seen in Figure 7, is possibly due to the presence of an interlayer slip in capillary tube flow. Since PPO–PS and LCP are immiscible, the rise in an interlayer slip is real possibility.[18] The calculations of the viscosity of the blends according to eq. (1) do not include the contribution of the interlayer slip. This contribution can be incorporated into the equation by introducing the interlayer slip factor, as proposed by Lin.[21] However, the problem exists in determining this coefficient.

Mechanical Properties

Figure 8 gives the typical stress–strain curve for 50/50 PPO–PS/LCP blend. This curve, along with the stress–strain curves obtained at other LCP concentrations (above 10%), indicates that the PPO–PS/LCP blends exhibit brittle fracture. Figures 9, 10, and 11 give, respectively, the tensile strength, secant modulus, and elongation to break as a function of LCP concentration in the blend. From Figure 9, it can be seen that there is an increase in the tensile strength with the increase in the LCP concentration in the blend. The increase in the tensile strength is minimal up to an LCP concentration of 40%, after which the increase is quite rapid. This increase in the strength of the immiscible blends can be attributed to the development of LCP fibers in the PPO–PS matrix. Figure 9 also gives a comparison of the tensile strength of PPO–PS/LCP blends with PPO/LCP blends studied by Limtasiri and Isayev.[16] It can be seen that the tensile strength values for PPO–PS/LCP blends are higher than those for PPO/LCP blends, particularly at low LCP concentrations, even though pure PPO shows higher tensile strength values than the PPO–PS alloy. This shows that the addition of even small quantities of LCP increases the tensile strength of the PPO–PS/LCP blends and decreases the tensile strength of the PPO/LCP blends. This can be attributed to better fiber formation of LCP in the blend in the case of PPO–PS/LCP blends, as shown by the morphology studies discussed later. The interfacial adhesion between the matrix polymer and the LCP fibers may be presumed

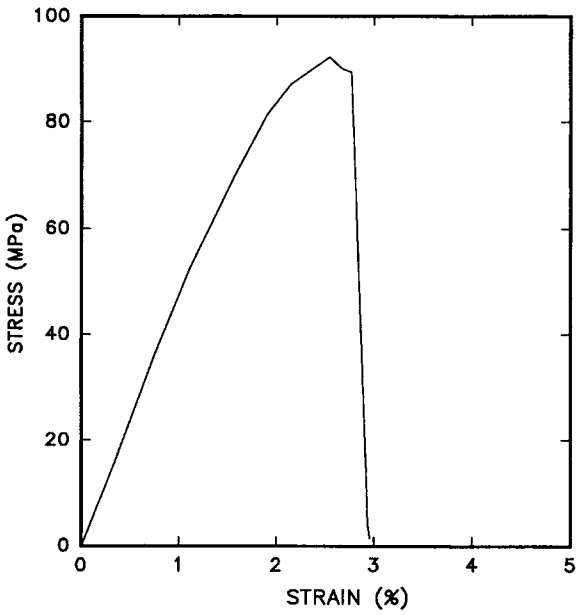

Figure 8 Stress–strain curve for the injection molded MTBs of 50/50 PPO–PS/LCP blends.

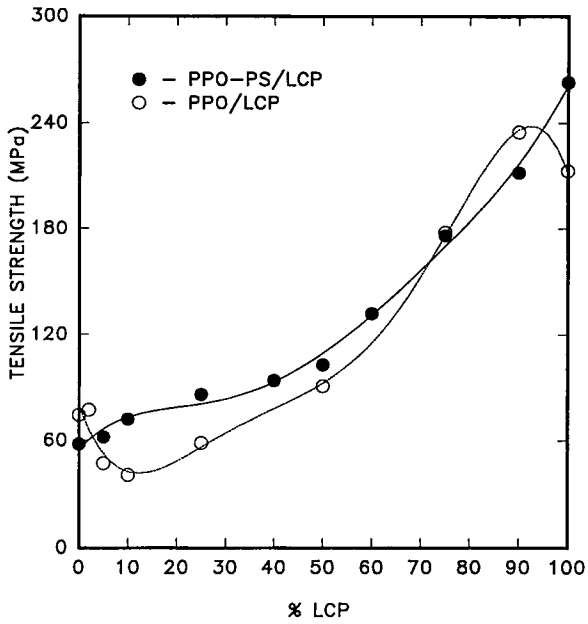

Figure 9 Tensile strength vs. LCP concentration for injection molded MTBs of PPO–PS/LCP. The hollow circles indicate the values obtained by Limtasiri and Isayev[16] for PPO/LCP blends.

to be greater in the case of PPO–PS than in the case of PPO. This possibility of better interface is also indicated by a slight shift of T_g of PPO–PS in the blends seen in Figures 3 and 4. This may lead to higher strength due to better reinforcement. Interestingly, the tensile strength of pure LCP in our study is somewhat higher than in the case of Limtasiri and Isayev.[16] This may be due to the lower processing temperature in our study (275°C), compared to 310°C in the case of studies by Limtasiri and Isayev.[16] At lower temperature, the viscosity of the LCP is higher and this may lead to higher frozen-in orientation in LCP molding. This may also be a reason for the higher strength of the PPO–PS/LCP blends.

Figure 10 gives the secant modulus of the PPO–PS/LCP blends as a function of LCP concentration in the blend, and also shows the secant modulus of PPO/LCP blends obtained from the Limtasiri and Isayev studies.[16] The secant modulus is a measure of the load-bearing capacity of the sample, particularly at small elongations, which is often applied to engineering thermoplastics.[5] Secant modulus significantly increases with increase in LCP concentration, up to 30% LCP concentration. Then it levels off up to 40% LCP concentration. From then on the values increase rapidly. The values obtained for

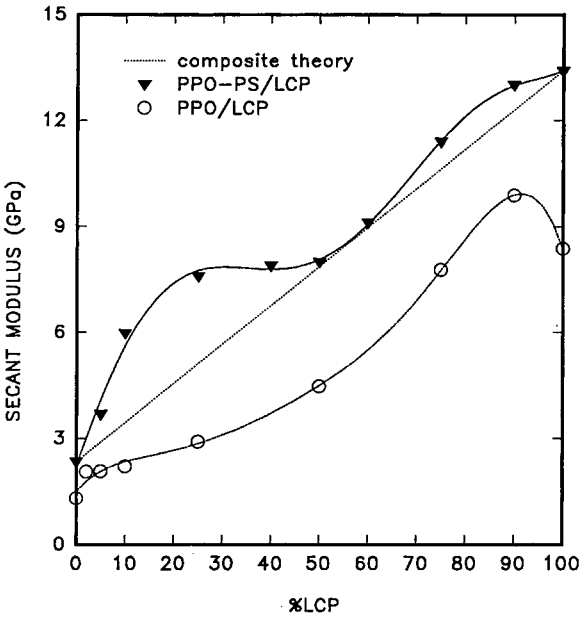

Figure 10 Secant modulus vs. LCP concentration for injection molded MTBs of PPO–PS/LCP blends. The hollow circles indicate the values obtained by Limtasiri and Isayev[16] for PPO/LCP blends. The dotted line represents the theoretically predicted values from the composite theory (eq. 2).

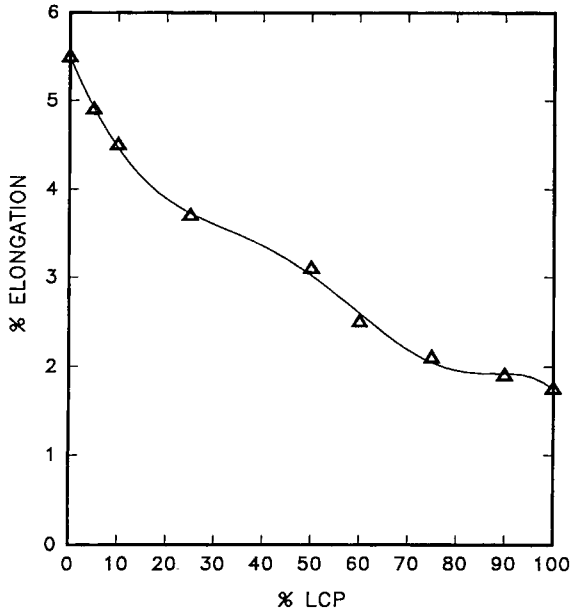

Figure 11 Elongation to break vs. LCP concentration for the injection molded MTBs of PPO–PS/LCP blends.

PPO–PS/LCP are significantly higher than those for PPO/LCP.[16] The figure also shows a comparison of experimental values and calculated values obtained from the composite theory. In these calculations it is assumed that the modulus of fibers is equal to the modulus of pure LCP in bulk. It can be seen that the actual and calculated values corroborate for the blends of LCP concentration around 50–60%, but there is a synergistic increase in the actual values for all other concentrations. The composite theory used is based on the rule of mixtures[22] and can be described as follows:

$$E_c = E_f V_f + E_m(1 - V_f) \qquad (2)$$

where E_c, E_f, and E_m are the modulus values for the composite, fiber, and matrix polymer, respectively, and V_f is the volume fraction of the fibers present in the matrix. The theory's assumption is that the reinforcing fibers are arranged uniformly and throughout the matrix. This does not happen in the case of PPO–PS/LCP blends where the skin region has more fibers than the core region for lower concentration of LCP, as seen in the morphology studies described later. Again, the interfacial adhesion between the matrix and the fibers may also significantly affect the modulus values; this is not accounted for by the composite theory. When compared with the modulus obtained for PPO/LCP blends, the values for PPO–PS/LCP blends are significantly higher. Thus the LCP reinforcement has a more prominent effect in the latter case.

Figure 11 gives the elongation-to-break of PPO–PS/LCP blends as a function of LCP concentration. PPO–PS has a high elongation-to-break. Samples with very low concentrations of LCP show a necking phenomenon, the neck region changing color to white during testing. As the fiber content increases, the elongation decreases.

Figure 12 gives the impact strength of the PPO–PS/LCP blends as a function of LCP concentration in comparison with that of the PPO/LCP blends taken from Limtasiri and Isayev.[16] The general trend, as seen from the figure, is that the impact strength increases with increased LCP concentration. However, at LCP concentrations up to 25%, there is a decrease in the impact strength with the increase in LCP concentration. From the figure it can be seen that the impact strength for PPO/LCP blends increases until 10% LCP concentration, then decreases and increases again with the increase in the LCP concentration. However, the values obtained for PPO–PS/LCP blends are far greater than those of the PPO/LCP blends. The decreased impact strength at low LCP concentrations can be attributed to the disturbance of a close and dense polymer matrix by the insertion of small amount of LCP fibers. The transfer of energy is mainly facilitated by a dense matrix. This energy transfer may be disturbed by the LCP fibers that are short, leading to poor energy distribution. At higher LCP concentrations, the fibers tend to elongate to a great extent and also start to bundle up. Now the energy supplied to the system may be propagated through the rigid, slender, and long fibers whose surface-to-volume ratio (L/D) favors the energy distribution. This may lead to much less residual energy available for the crack propagation and hence the impact strength may be higher. Similar observations have been noted for PEEK/LCP blends.[6]

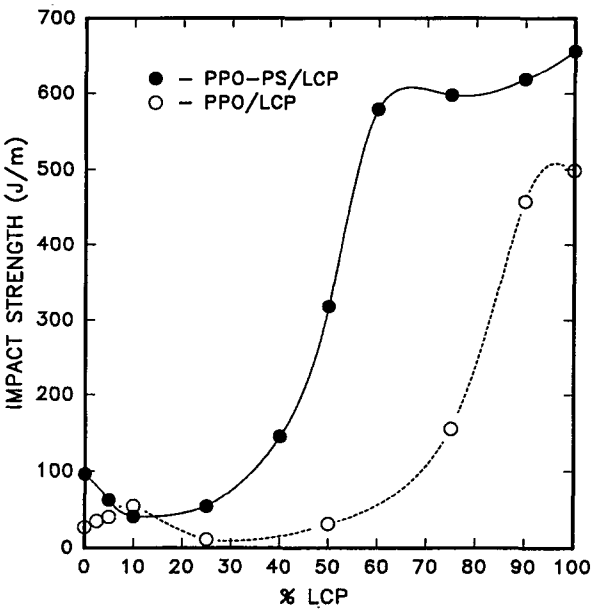

Figure 12 Impact strength vs. LCP concentration for the injection molded MTBs of PPO–PS/LCP. The hollow circles indicate the values obtained by Limtasiri and Isayev[16] for PPO/LCP blends.

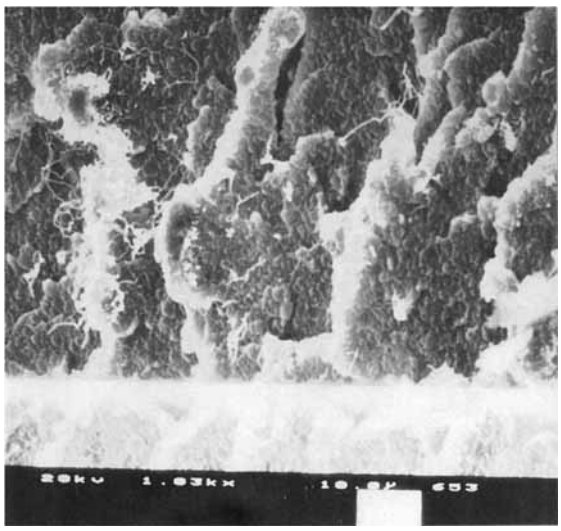

Figure 13 SEM micrograph of injection molded MTBs of PPO/PS alloy.

Morphological Characteristics

Morphological studies on PPO–PS/LCP blends have been undertaken to correlate the mechanical properties of the blends and to study the nature of fiber formation. The morphology of the blends depends on the composition, shear rate, and location of the crosssection.[8,12] It has been known that the elongational flow leads to LCP fiber formation in the case of thermoplastic/LCP blends. The aspect ratio of these fibers depends on the extent of elongational flow provided. Figure 13 shows the morphology of pure PPO–PS alloy. There is no distinction between the PPO and PS phases, owing to the two phases' complete miscibility. The evenness of the density of the matrix alloy may be the reason for the superior performance of PPO–PS alloys as engineering thermoplastics.

As in the case of other thermoplastics/LCP blends,[1,9,10] blends of PPO–PS/LCP show distinct skin–core morphology. Figure 14 shows the skin (a) and the core (b) regions of PPO–PS/LCP blend with 10% LCP concentration. The emergence of LCP in the domain of PPO–PS is visible in this case. The

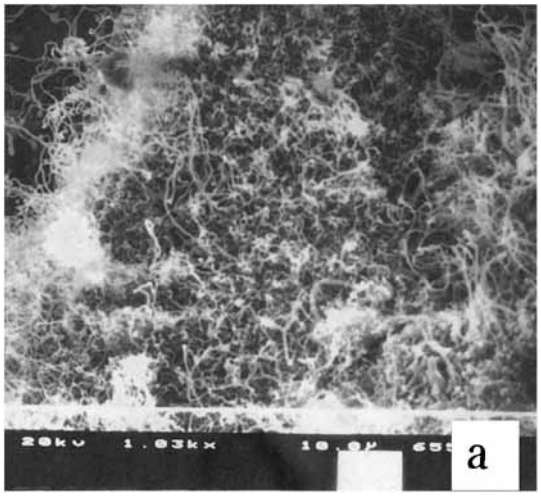

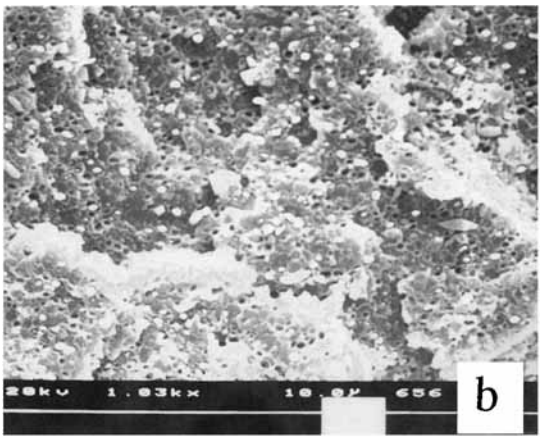

Figure 14 SEM micrographs of (a) skin and (b) core regions of injection-molded MTBs of 90/10 PPO–PS/LCP blends.

development of skin–core morphology can be attributed to the fountain flow during the injection molding process. This type of flow leads to the contact of the melt, highly elongated in the melt front region, with the cold surface of the mold and velocity rearrangement results due to this.[23] The skin region consists of very small intertwined LCP fibers. The core region exhibits the PPO–PS morphology with small LCP microfibers embedded in it.

Figure 15 shows the skin (a) and the core (b) regions for the PPO–PS/LCP blends with 25% LCP concentration. Here the LCP fibers are more developed in the skin region and the fibers are bundled up into sheets placed adjacent to each other. There is a clear distinction between the morphologies of the skin and core regions, though the core region contains some LCP fibers embedded in it. The presence of a strong skin region may be responsible for the better mechanical properties.

Figure 16 shows the skin (a) and the core (b) regions for the blends with 40% LCP concentration. The skin region shows a more complete ordering of the sheets of the LCP fibers. The thickness of these sheets is lesser and the orientation toward the machine direction is greater when compared with the morphology of the 25% LCP-concentration blends. The layered structure in the skin layer may be attributed to the expanding radial flow at the gate, the fountain flow of the advancing melt, and the nonisothermal shear flow of the hot melt into a colder cavity.[24] At this concentration of LCP in the blend, there seems to be LCP present in the core region, although fibers are less apparent. T. Sun et al.[25] have

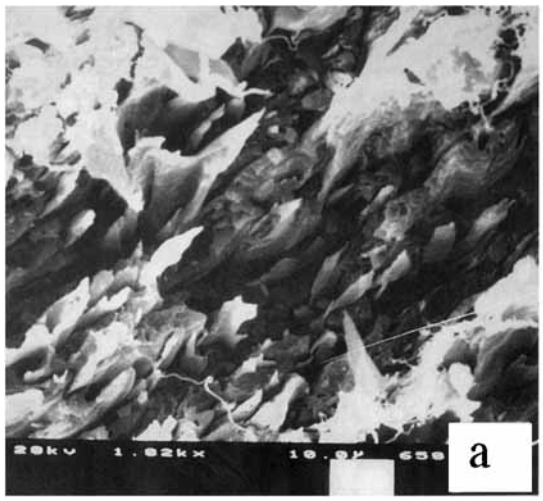

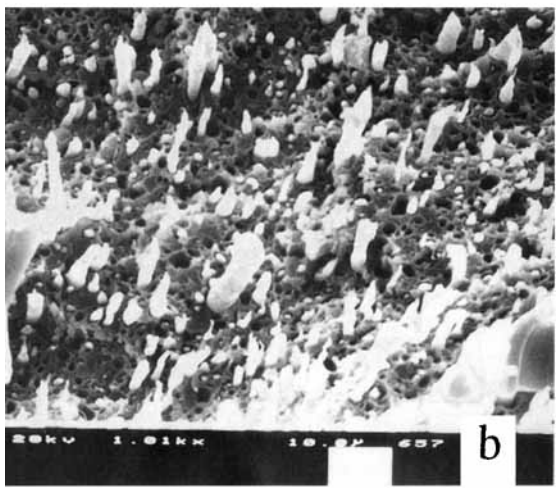

Figure 15 SEM micrographs of (a) skin and (b) core regions of injection molded MTBs of 75/25 PPO–PS/LCP blends.

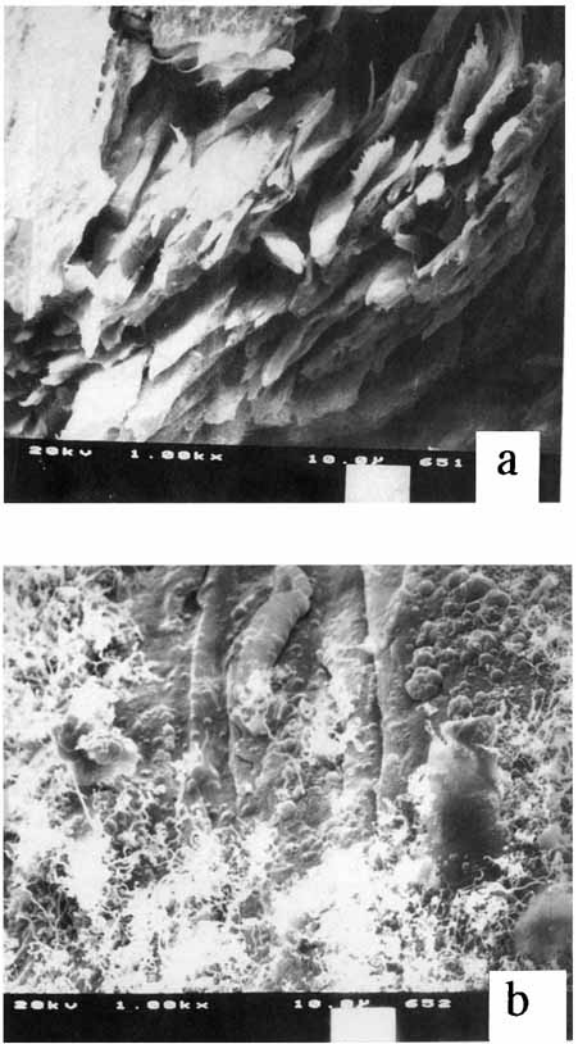

Figure 16 SEM micrographs of (a) skin and (b) core regions of injection molded MTBs of 60/40 PPO–PS/LCP blends.

observed that for a PEI/LCP system, at an LCP concentration of around 50%, the LCP fibers seem to retract to a droplet morphology. A consequential reduction in mechanical properties for these blends has been observed. In our earlier work on PEI/LCP blends,[7] the fibers were distinctly present at this concentration of LCP. In this case the plateau of properties was not seen. In the present study, at concentrations of 40% LCP, this phenomenon of reduction of fibers is clearly manifest, as seen in Figure 16. In the case of PS/LCP blends,[26] a profusion of fibers in the core region has been observed. Analysis by Ganthier,[27] based on the theory by Chaffey et al.[28] has shown that there exists a lateral migration of the deformed liquid drops in the viscoelastic fluids toward the tube axis; while in pseudoplastic liquids, the droplets attain an equilibrium position between the wall and the axis of the tube. In the latter case, a two-way migration occurs. Droplets initially migrate towards the wall. When the flow rate is increased, the inward migration becomes predominant and the equilibrium is pushed towards the axis. This may be the reason for the appearance of fibers in the core region seen in Figure 17(b). When compared to the PPO/LCP blends,[16] the PPO–PS/LCP blends have more fibers in the core region and they are also more uniformly distributed at this concentration of LCP. This may be the reason for higher mechanical properties, particularly the impact strength.

Figure 18 shows the skin (a) and the core (b) regions for the PPO–PS/LCP blends with an LCP

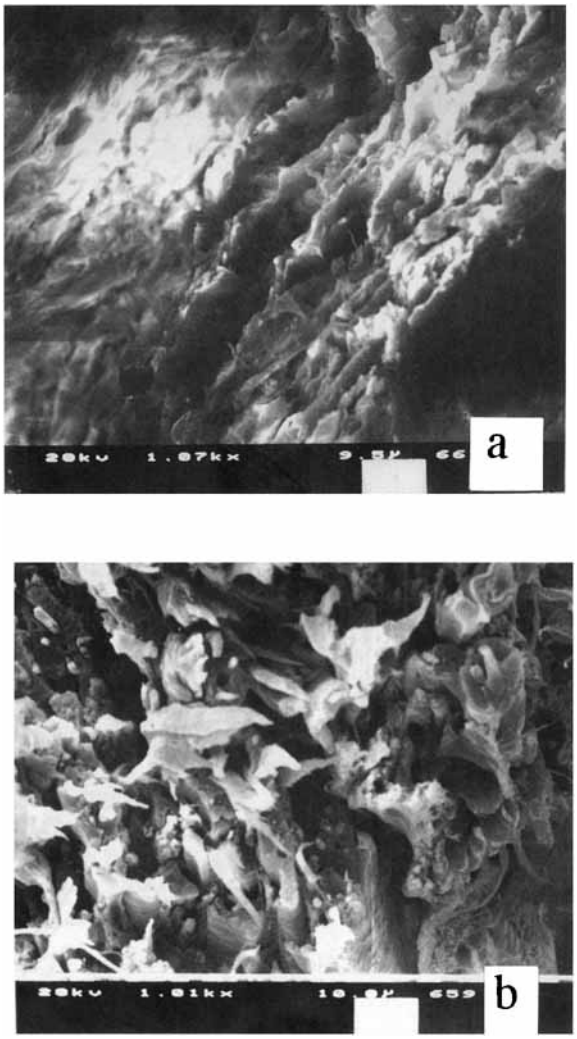

Figure 17 SEM micrographs of (a) skin and (b) core regions of injection molded MTBs of 50/50 PPO–PS/LCP blends.

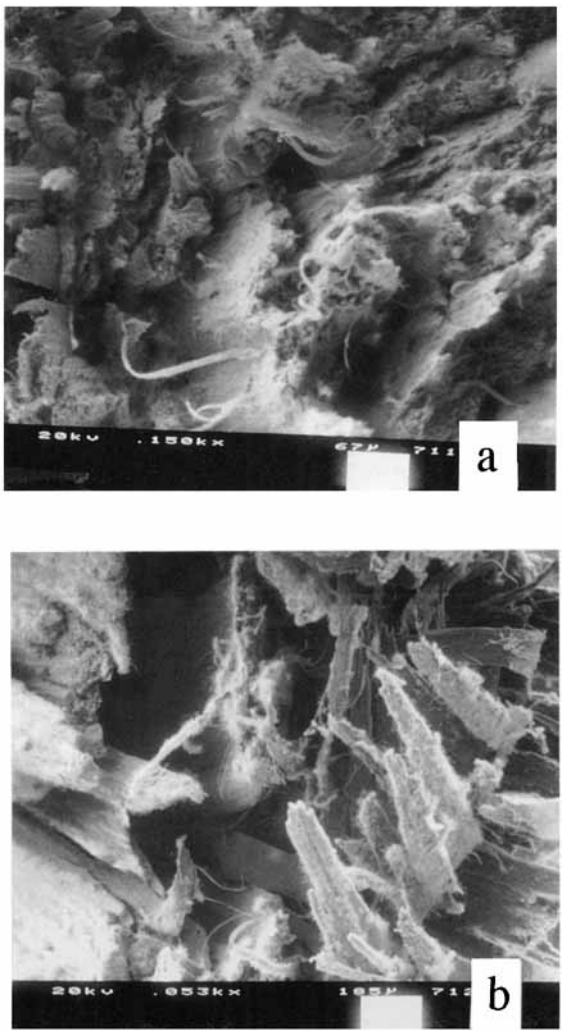

Figure 18 SEM micrographs of (a) skin and (b) core regions of injection molded MTBs of 25/75 PPO–PS/LCP blends.

concentration of 75%. It can be seen that there are no perceptible skin and core regions. The SEM photomicrographs also show that LCP is the dispersed phase and PPO–PS is the continuous phase. In the other words, even at 75% LCP concentration the blends do not show a phase reversion. The skin area shows distinct and discrete bundles of LCP, and so does the core region. This accounts for the very high mechanical properties. Similar morphologies exist for LCP concentrations above 75%. Thus the mechanical properties observed are also close to that of pure LCP processed at the same temperature.

CONCLUSIONS

The miscibility, rheology, mechanical properties, and morphology of the PPO–PS/LCP blends with various concentration of LCP have been studied. It has been seen that the PPO–PS alloy and the LCP are immiscible and incompatible at all LCP concentrations in the blend. It has also been seen that the addition of even small amounts of the LCP to the alloy decreases its viscosity. The LCP thus acts as a processing aid for the PPO–PS alloy. Also, the injection-molded samples of the PPO–PS/LCP blends have been found to have a PPO–PS matrix in which the LCP forms *in situ* reinforcing fibers. The mechanical properties of the blends show a tremendous improvement when compared with those of pure PPO–PS, and this has been attributed to the *in situ* LCP fiber reinforcement. The morphological studies performed on these blends indicate that there exists a skin–core morphology for the blends, particularly at low LCP concentrations. As the concentration increases, the LCP fibers become longer and packed together. This is attributed as a reason for enhanced mechanical properties. The studies show that the LCP could be used as a processing aid and an *in situ* reinforcing agent for the thermoplastic under suitable processing conditions. This study reveals the possibility of using the LCP as a suitable reinforcing agent for other engineering thermoplastics, for a wide range of applications where the strength of the composite is important.

This work is partially supported by a grant from the Edison Polymer Innovation Corporation.

REFERENCES

1. D. Dutta, H. Fruitwala, A. Kohli, and R. A. Weiss, *Polym. Eng. Sci.*, **30,** 1005 (1990).
2. A. I. Isayev and T. Limtasiri, in *International Encyclopedia of Composites,* Vol. 3, S. M. Lee, Ed., VCN Publishers, New York, 1990, p. 55.
3. V. G. Kulichikhin and N. A. Plate, *Polym. Sci. USSR.*, **31,** 459 (1991).
4. S. S. Bafna, J. P. De Souza, T. Sun, and D. G. Baird, *Polym. Eng. Sci.*, **13,** 808 (1993).
5. G. Kiss, *Polym. Eng. Sci.*, **27,** 410 (1987).
6. A. Mehta and A. I. Isayev, *Polym. Eng. Sci.*, **13,** 971 (1991).
7. A. I. Isayev and S. Swaminathan, in *Adv. Composites III, Expanding Technology,* ASM 259, 1987.
8. D. Beery, S. Kenig, and A. Siegmann, *Polym. Eng. Sci.*, **31,** 451 (1991).
9. A. Siegmann, A. Dagan, and S. Kenig, *Polymer,* **26,** 1325 (1985).
10. E. G. Joseph, G. L. Wilkes, and D. G. Baird, *Polym. Prepr., Am. Chem. Soc., Div. Polym. Chem.,* **(2)24,** 304 (1983).
11. G. Crevecoeur and G. Groeninckx, *Polym. Eng. Sci.*, **33,** 15 (1993).

12. A. I. Isayev and M. Modic, *Polym. Compos,* **8,** 158 (1987); U.S. Patent 4,728,698, 1988.
13. F. N. Cogswell, B. P. Griffin, and J. B. Rose, U.S. Patent 4,386,174, 1981.
14. J. R. Fried, W. J. MacKnight, and F. E. Karasz, *J. Anal. Phys.,* **50,** 6052 (1979).
15. J. Throne and R. C. Proghelof, *Design Properties of Polymers,* Sherwood Tech. Inc., Akron, Ohio, 1988.
16. T. Limtasiri and A. I. Isayev, *J. Appl. Polym. Sci.,* **42,** 2923 (1991).
17. A. I. Isayev and P. R. Subramanian, *Polym. Eng. Sci.,* **32,** 85, 1992.
18. C. K. Shih, *Polym. Eng. Sci.,* **16,** 328 (1976).
19. M. V. Tsebrenko, M. V. Jacob, M. Yu Kuchinka, A. V. Yudin, and G. V. Vinogradov, *Int. J. Polym. Mater.,* **3,** 99 (1974).
20. R. F. Heitmiller, R. Z. Maar, and H. H. Zabusky, *J. Appl. Polym. Sci.,* **8,** 873 (1964).
21. C. C. Lin, *Polym. J.,* **11,** 185 (1979).
22. A. Kelly and W. Tyson, *J. Mater. Sci.,* **7,** 1315 (1971).
23. A. I. Isayev, Ed., *Injection and Compression Molding Fundamentals,* Marcel Dekker, New York, 1987.
24. S. Garg and S. Kenig, in *Strength and Stiffness of Polymers,* R. S. Porter and A. E. Zacharides, Eds., Marcel Dekker, New York, 1988.
25. T. Sun, D. G. Baird, H. H. Huang, D. S. Done, and G. L. Wilkes, *J. Compos. Mater.,* **25,** 788 (1991).
26. R. A. Weiss, W. Huh, and L. Nicolais, *Polym. Eng. Sci.,* **27,** 684 (1987).
27. F. Ganthier, G. L. Wilkes, and S. G. Mason, *Trans. Soc. Rheol.,* **15,** 297 (1971).
28. C. E. Chaffey, M. Brenner, and S. G. Mason, *Rheol. Acta,* **4,** 64 (1965).

Received March 25, 1994
Accepted August 17, 1994